Synergy between 1-D and 3-D radiation transfer models to retrieve vegetation canopy properties from remote sensing data

B. Pinty, N. Gobron, J.-L. Widlowski, T. Lavergne, and M. M. Verstraete

Global Vegetation Monitoring Unit, Institute for Environment and Sustainability, European Commission Joint Research Centre, Ispra, Italy

Received 9 July 2004; revised 2 September 2004; accepted 16 September 2004; published 6 November 2004.

[1] We devise a computer efficient and flexible inversion technique to retrieve vegetation canopy parameters, in particular the Leaf Area Index, from the radiance field emerging at the top of a structurally heterogeneous systems overlying an anisotropic spatially uniform surface background. The proposed inversion strategy focuses on a reanalysis of multiangle and multispectral measurements unhindered by the many specific constraints imposed by the operational application of the current algorithms and their associated limitations on data staging. This technique capitalizes on the decoupling between contributions due to the canopy only and those invoking the background reflectance properties. These contributions are decomposed into the wavelength dependent and independent contributions. A quasi-linear relationship is thus obtained between the radiance/reflectance emerging from the top of the canopy layer and the background reflectance. Although all individual contributions can be estimated from accurate three-dimensional radiation transfer models, we propose appropriate approximations in order to estimate the minor terms. These approximations exploit the relatively limited dependency exhibited by these relatively smaller contributions with respect to the azimuthal coordinate. Moreover, additional mathematical developments are proposed to further approximate these terms by their corresponding solutions obtained in the limit case of a plane-parallel turbid medium scenario. They require defining effective values of the state variables entering the plane-parallel turbid medium model. The resulting reflectance of a three-dimensional spatially heterogeneous vegetation layer is driven by a sum of contributions that can be precomputed offline on the basis of the three-dimensional and plane-parallel homogeneous turbid medium model capabilities. The decoupling of the intrinsic vegetation and the background contributions allows many of the contributions to be precomputed and stored in look-up tables. This development yields a simple and computer efficient inversion scheme that allows us to jointly retrieve the values of the main vegetation layer attributes and the underlying background radiative properties. Demonstration tests based on actual multiangular and multispectral data set are currently being investigated. *INDEX TERMS:* 0315 Atmospheric Composition and Structure: Biosphere/atmosphere interactions; 0320 Atmospheric Composition and Structure: Cloud physics and chemistry; 0360 Atmospheric Composition and Structure: Transmission and scattering of radiation; 0933 Exploration Geophysics: Remote sensing; *KEYWORDS:* vegetation canopy, radiation transfer, inversion

Citation: Pinty, B., N. Gobron, J.-L. Widlowski, T. Lavergne, and M. M. Verstraete (2004), Synergy between 1-D and 3-D radiation transfer models to retrieve vegetation canopy properties from remote sensing data, *J. Geophys. Res.*, *109*, D21205, doi:10.1029/2004JD005214.

1. Introduction

[2] The Leaf Area Index (LAI) of a vegetation canopy is a quantitative measure of the amount of leaf material contained in a given canopy volume. The LAI is generally defined as the total one-sided area of all leaves in this canopy volume, or sometimes the area-projected in the case of needleleaf canopies, reported per unit ground surface, and is thus a nondimensional quantity (m^2 m^{-2}). Specifically, the total or cumulative LAI of a canopy is the sum, throughout the canopy depth, of all canopy layer contributions. The LAI of each of the contributing canopy layers is itself simply given by the sum of the leaf areas within the layers per unit ground surface.

0148-0227/04/2004JD005214$09.00

[3] This volume-integrated definition for LAI does not specify any constraints on the actual distribution of the leaves in the canopy volume of interest. Consequently, any given LAI value (representing a fixed number of leaves) corresponds to a very large number of possible leaf distributions (position, orientation, number and size) in the three-dimensional (3-D) space. The number of such possible distributions should, intuitively, increase with the size of the canopy volume and, more particularly, with the horizontal width of this volume since the volume height is somewhat bounded to a few tens of meters. The 3-D spatial distribution of the leaves is itself controlled by multiple factors including plant functional type, plant phenology, climatic conditions and anthropogenic activities, to name but a few. The plant functional type may to some extent restrict the range of spatial organization that can be encountered over a hierarchy of spatial scales, going from the leaf clumps (a few tens of centimeters) to the stand level (a few hundred meters) and even more in the case of large regions likely to exhibit complex yet organized heterogeneous land cover.

[4] In actual situations, local (tree level) LAI values can vary spatially by an order of magnitude within the instantaneous field of view of medium resolution sensors (a few hundred meters) that collect radiance measurements most likely to be application relevant for the assessment of LAI at the desired spatial and temporal resolutions over the globe. Unfortunately, the intra-pixel variability within the instantaneous field of view of medium resolution sensors strongly affects the radiation transfer regime in structurally complex canopies [e.g., *Gerard and North*, 1997; *Knyazikhin et al.*, 1998a; *Panferov et al.*, 2001; *Widlowski*, 2002; *Rautiainen et al.*, 2004]. Given the level of complexity, it remains quite a challenging task to simulate accurately the radiation transfer regime into structurally and optically complex vegetation systems without using stochastic or Monte-Carlo ray tracing models [*Pinty et al.*, 2004].

[5] The accurate retrieval of canopy structural information, in particular LAI, from medium resolution sensors is further hindered by the lack of accurate a priori knowledge of the radiation transfer properties of the underlying background surface (e.g., soil, snow, water, undergrowth), namely, the surface Bidirectional Reflectance Factor (BRF). This issue is typical of the inverse problem since the optical thickness of an absorbing/scattering structurally homogeneous/heterogenous medium can be retrieved accurately only if the boundary conditions, including the lower ones, are (assumed to be) known a priori or can be jointly assessed during the retrieval.

[6] The importance of both vegetation structure and the upper and lower boundary conditions to the radiation transfer in vegetation canopies has been recognized in the design of both experimental and operational inversion techniques aiming to retrieve simultaneously LAI and background brightness [e.g., *Gobron et al.*, 1997a; *Pinty et al.*, 1998; *Knyazikhin et al.*, 1998b]. The current implementation of the MODIS/MISR LAI retrieval algorithm constitutes a recent example of such an approach dedicated to the operational interpretation of data collected over the globe [*Knyazikhin et al.*, 1998c]. The nominal version of this algorithm exploits the well-known wavelength-independent behavior of the optical thickness of the medium [e.g., *Ross*, 1981; *Knyazikhin and Marshak*, 1991; *Pinty and Verstraete*, 1998; *Knyazikhin et al.*, 2004]. In short, the algorithm solves the radiation transfer problem for LAI given a predefined set of six structural vegetation types distributed over the globe, as well as and some typical preset values of leaf reflectance/transmittance and background properties [*Knyazikhin et al.*, 1998c]. The operational nature of the MISR and MODIS LAI algorithms imposed constraints (computational cost, algorithmic robustness, and data staging) on the solutions of this ill-posed and badly conditioned inversion problem. These constraints limit to some extent the scientific strategy adopted to implement this algorithm in a ground segment. An interesting aspect of the MISR and MODIS algorithms is the selection of solutions based on the analysis of radiant fluxes which forces the solutions to satisfy the energy conservation and, in the mean time, limits very significantly the size of the look-up tables (LUTs) to be maintained by the ground segments.

[7] The strategy adopted here recognizes some of these computational constraints but also takes full advantage of the capability of 3-D radiation transfer models to accurately represent the radiation transfer regime in structurally complex canopies. By focusing on the task of reanalyzing historical archives of remote sensing observations, the approach proposed below can take advantage of (1) the potential offered by 3-D radiation transfer models to simulate accurately individual components of the radiation transfer regimes in vegetation canopies of arbitrary complexity and (2) the possibility to explicitly represent the role and impact of the background properties in a computationally economic way. The overall strategy is based on the identification of the various contributions to the total solution with a view to decouple the intrinsic aborption/scattering effects in the vegetation layer from those due to the lower boundary condition representing the anisotropic background. In developing this approach we have been inspired by the achivements of the cloud science community and this, in turn, suggests that some of the developments proposed below in the context of plant canopies may also be relevant to solve similar problems in other geophysical systems.

[8] With the help of a few reasonable hypotheses, the overall reflectance of a complex heterogeneous canopy over a background of arbitrary brightness and anisotropy can be expressed quasi-linearly as the sum of a contribution due to the canopy alone and the others due to the background. The departure from linearity originates from the effect of multiple scattering between the canopy and the background. In the process, the significant contributions dominated by vegetation structure will be estimated using 3-D models, such as Monte-Carlo ray-tracing codes, while minor contributions will be evaluated using models suited for plane-parallel turbid medium theory whenever appropriate. These approximations are required in order to solve dynamically, during the retrieving process the coupling between the LAI of the structurally heterogeneous vegetation layer and its lower boundary condition characterized by the anisotropic surface background. The application of this technique against current multispectral and multiangular measurements collected from spaceborne sensors is currently

undertaken, with special attention to documenting the uncertainties associated to the retrievals.

2. Representation of Geophysical Scenes for Medium Resolution Sensors

2.1. Definition of the "Radiatively Independent Volume"

[9] To establish the radiation transfer equations required to solve the inverse problem, it is necessary to define a plane of reference at the top of the absorbing-scattering layer under investigation. This plane permits us to define relevant radiation quantities within this layer as well as at the upper boundary conditions. One of these corresponds to the radiance emerging from this layer that can be estimated or derived from remotely sensed measurements. Since the bottom of the layer can be defined as well, e.g., the soil background level for a canopy vegetation problem, this upper reference plane, defined irrespective of the geophysical properties of the layer in terms of spatial heterogeneity, thus allows the delineation of an absorbing-scattering volume including all geophysical entities of relevance, e.g., the tree crowns and the woody elements. The most simple situation is therefore the one involving a volume bounded by two parallel planes at the top and the bottom. This volume can then be filled up by elementary scatterers, defining elementary scattering volumes, e.g., individual leaves or vegetation clumps in the case of plant canopies, that can be distributed in a spatially explicit manner in 3-D space following a variety of distribution laws, including, Poisson, Gamma distributions, fractal amongst others [e.g., *Nilson*, 1971; *Oker-Blom and Kellomaki*, 1983; *Cescatti*, 1988; *Prusinkiewicz and Lindenmayer*, 1990; *Borel et al.*, 1991; *Nilson*, 1991; *Welles and Norman*, 1991; *Govaerts*, 1996; *Widlowski et al.*, 2001].

[10] The horizontal extent of the volume that encloses the elementary scattering volumes can itself be defined so that the modeling of the radiation transfer regime into this volume as well as the finding of solutions to the inverse problem is made as simple as possible. In that context, it is crucial to estimate the lateral extent of the volume beyond which the net effects due to photon horizontal transport can be neglected at any level of this volume [e.g., *Titov*, 1990, 1998; *Szczap et al.*, 2000; *Tian et al.*, 2002; *Widlowski*, 2002; *Marshak and Davis*, 2004]. In other words, if the lateral extent of the volume is large enough to ensure that the contribution due to the net radiant horizontal fluxes is negligible at any level with respect to the vertical fluxes, then the measured radiance from each pixel is radiatively independent from the radiation transfer regime prevailing in the surrounding regions. This "radiatively independent volume" thus satisfies a domain-averaged conservation law that is such that the sum of the vertical fluxes associated to reflectance, transmittance and absorptance factors is essentially equal to unity. When such conditions are satisfied, the inversion procedures can be applied on a pixel per pixel basis, that is, for all practical purposes, with no need to describe and to account for the radiation transfer regime of the surrounding pixels, at any spatial resolutions lower than the one defined by the size of this "radiatively independent volume."

[11] The size of the "radiatively independent volume" thus depends on the location, number and radiation properties (e.g., absorption efficiency and preferred direction of scattering) of the elementary scattering volumes in the 3-D space, as well as on the scattering properties prevailing at the bottom of the layer, i.e., the BRF of the lower boundary condition. For all practical purposes, the lower limits of this "radiatively independent volume," corresponding to the highest spatial resolutions suitable for inversion, can be estimated from a wide variety of 3-D radiation transfer simulations [e.g., *Widlowski*, 2002; *Marshak and Davis*, 2004]. These limits can as well be estimated from the analysis of power spectra of radiances measured over a range of geophysical conditions at a very high spatial resolution. In this latter case, the limit could be taken as a multiple of the wavenumber where scale breaks occur due to radiative smoothing, for example [e.g., *Cahalan and Snider*, 1989; *Marshak et al.*, 1995; *Oreopoulos et al.*, 2000].

2.2. Characterization of the Geophysical Medium Inside the Radiatively Independent Volume

[12] Once these geometrical limits are established, the "radiatively independent volume" can be populated with absorbing/scattering elements that best mimic situations actually encountered on Earth. To achieve this goal, it is appropriate to capitalize on existing knowledge regarding not only the optical properties of the various elements entering the volume, but also their distribution in 3-D space. Such a knowledge is (1) strongly dependent on the biome type, (2) often sparsely distributed in the literature, and (3) rarely assembled in a coherent manner (for instance, the estimates of allometric equations and their relationships with LAI per tree crown). The task is obviously rendered very complex and arduous due to the natural variability of the surface systems. An attempt to present this structural information based on current knowledge has been recently published by *Widlowski et al.* [2003] for a limited set of tree species found over the boreal regions. Such systems are of significant interest for a variety of reasons including the large uncertainties in the carbon cycle estimates [e.g., *Rayner et al.*, 1999; *Knorr and Heimann*, 2001; *Gurney et al.*, 2002] associated with the boreal regions as well as for the monitoring of various land use and land cover changes that occur, for instance, in the Northern Eurasian sector.

[13] *Widlowski et al.* [2003] provide relevant structural information to generate typical scenes for five European tree species that can be ingested by a 3-D ray tracing Monte-Carlo model. Thus it is possible to simulate the full radiation transfer regime and the associated radiance fields emerging from both the top and the bottom of the canopy layer for any background conditions. For all practical purposes, and given the context of the present study, it is useful to distinguish between the following sets of variables used to characterize the generated scenes:

[14] 1. A given vegetation or biome type is selected first (for example, any one of the five European tree species documented in *Widlowski et al.* [2003] is assumed to correspond to a biome type). This already imposes a series of properties such as the distribution in size and shape of the tree crowns, the allometric equations used to generate height distribution functions and associated leaf area density per

crown to name but a few. In the rest of this paper, the ensemble of "hidden"vegetation attributes corresponding to each biome type will be noted by a vector **B**.

[15] 2. Having identifed a biome type, we then have to populate the "radiatively independent volume" with individual (or ensemble of) scatterers. For instance, we have to select tree density values for each given scenario and to spatially allocate the trees in the 2-D space. This step ends up with as many scenes as needed, corresponding to multiple vegetation structure conditions. The ensemble of parameters associated to this task, except the LAI that is kept free, are regrouped into a vector noted **S** in the rest of this paper.

[16] 3. Last but not least, the spectral properties of all canopy elements are specified by a vector **O**. They largely control the radiation transfer regimes. Optical plant properties are not always well known (in particular for coniferous trees) partly due to the technical difficulty of acquiring these measurements and partly because of the high number of existing species. This particular grouping of the variables describing the scenes of interest is driven by the application at hand: a different choice might be more appropriate in a different context. However, the three sets described above permit us to generate sets of vegetation scenes exhibiting a wide range of variability in key environmental variables such as LAI, fractional vegetation cover, as well as, for instance geometrical information (average canopy height versus mean tree interdistance) proved essential to conduct a variety of applications [*Widlowski et al.*, 2004].

3. Modeling the Radiance Field Backscattered by Structurally Heterogeneous Systems

3.1. Identification of the Main Contributions

[17] The radiance field emerging from the top of a canopy layer enclosed into a "radiatively independent volume" can always be decomposed into a sum of terms isolating the contributions due to scattering processes involving the background, the direct and the diffuse radiances, as is commonly done in various fields of geophysics [e.g., *Chandrasekhar*, 1960; *Lenoble*, 1985; *Liou*, 1980]:

$$I^{\uparrow total}_{coupled}(z_{toc},\Omega,\Omega_0) = I^{\uparrow Coll}_{veg}(z_{toc},\Omega,\Omega_0) + I^{\uparrow UnColl}_{bgd}(z_{toc},\Omega,\Omega_0) + I^{\uparrow Coll}_{bgd}(z_{toc},\Omega,\Omega_0) \quad (1)$$

where $I^{\uparrow total}_{coupled}(z_{toc}, \Omega, \Omega_0)$ denotes the radiance derived at the top of the vegetation canopy (z_{toc}) from an analysis of the data collected by a sensor observing along direction Ω, when the Sun is located in direction Ω_0. Here and in the rest of this paper, Ω stands for the couple zenith (which cosine is noted μ)/azimuth angles (noted ϕ) and the subscript 0 identifies the particular direction of the Sun. From now on, all physical variables appearing below a spectral integral are deemed to be monochromatic quantities and the downwelling (upwelling) radiances are identified by the symbols $\downarrow$ ($\uparrow$), respectively.

[18] The first term on the right-hand side of (1), $I^{\uparrow Coll}_{veg}(z_{toc}, \Omega, \Omega_0)$, is the contribution due to the radiation that has not interacted with the background but only with the canopy elements contained within the radiatively independent volume. This contribution corresponds to the "Black Background" solution to the radiation transfer problem ($I^{\uparrow total}_{coupled}(z_{toc}, \Omega, \Omega_0) = I^{\uparrow Coll}_{veg}(z_{toc}, \Omega, \Omega_0)$ in the case of a perfectly absorbing background). The "Black Background" expression is introduced instead of the traditional "Black Soil" because the soil is only one of the many possible backgrounds to the above vegetation canopy. One of the major geophysical variables of interest embedded within this contribution is the Leaf Area Index (LAI) of the scene. Formally, the "Black Background" contribution is thus expressed as $I^{\uparrow Coll}_{veg}(z_{toc}, \Omega, \Omega_0; \mathbf{B}, \mathbf{O}, \mathbf{S}, LAI_{scene})$.

[19] The second contribution, $I^{\uparrow UnColl}_{bgd}(z_{toc}, \Omega, \Omega_0)$, denotes the radiation that has traveled through the gaps of the canopy layer. It thus depends on the probability of finding gaps in the vegetation layer which are such that the collimated downward radiation from direction Ω_0 is intercepted by the background only, and then scattered back into the upward direction Ω without interception by the vegetation layer. This contribution is thus strongly controlled by the structural properties of the vegetation layer, i.e., the number, size and shape of the vegetation gaps, as well as the background BRF value, but not on the spectral properties of the phytoelements. Formally this "Black Canopy" contribution ($I^{\uparrow total}_{coupled}(z_{toc}, \Omega, \Omega_0) = I^{\uparrow UnColl}_{bgd}(z_{toc}, \Omega, \Omega_0)$ in the case of a perfectly absorbing canopy layer) is thus expressed as $I^{\uparrow UnColl}_{bgd}(z_{toc}, \Omega, \Omega_0; \mathbf{B}, \mathbf{S}, LAI_{scene}, BRF_{bgd})$ and, since only the Ω_0 for the downward direction and Ω for the upward direction matters, it can be expressed as follows:

$$I^{\uparrow UnColl}_{bgd}(z_{toc},\Omega,\Omega_0) = I^{\downarrow UnColl}_{bgd}(z_{bgd},\Omega_0)\rho_{bgd}(z_{bgd},\Omega,\Omega_0) \cdot T^{\uparrow UnColl}_{bgd}(z_{toc},\Omega) \quad (2)$$

where $I^{\downarrow UnColl}_{bgd}(z_{bgd}, \Omega_0)$ is the the direct radiation reaching the background level and $T^{\uparrow UnColl}_{bgd}(z_{toc}, \Omega)$ is the direct transmission of this uncollided radiation available at level z_{bgd} in the upward direction Ω. The occurence of extinction at discrete locations in the vegetation layer is a major feature in plant canopy radiation transfer problem since it depends only on the size and shape of the free space between the elementary scattering elements. This feature gives rise to the well-known hot spot phenomenon and various theories and models have been proposed to account for this effect in the case of structurally homogeneous canopies [e.g., *Nilson and Kuusk*, 1989; *Marshak*, 1989; *Gerstl and Borel*, 1992; *Verstraete et al.*, 1990; *Kuusk*, 1991; *Jupp and Strahler*, 1991; *Knyazikhin et al.*, 1992; *Gobron et al.*, 1997b]. In the case of structurally heterogeneous canopies, the situation is made more complex due to the extreme diversity of possibilities to aggregate leaves into clumps and then to distribute them in the 3-D space available in the "radiatively independent volume." Nevertheless, as is the case for homogeneous conditions, various attempts have been made to express the probability of finding gaps in heterogeneous environments assuming probability distribution functions for the clumps [e.g., *Nilson*, 1991; *Strahler and Jupp*, 1991].

[20] The third term on the right-hand side of (1) expresses the coupled contribution due to the multiple interactions between the background and the vegetation layer. It thus formally depends on the entire set of geophysical properties describing the scene, namely, $I^{\uparrow Coll}_{bgd}(z_{toc}, \Omega, \Omega_0; \mathbf{B}, \mathbf{O}, \mathbf{S}, LAI_{scene}, BRF_{bgd})$. This contribution can be decomposed

into two components to distinguish the contribution due to the radiation singly collided by the background before or after being scattered at least once by the vegetation layer, and the remaining multiply collided contribution between the vegetation layer and the background:

$$I_{bgd}^{\uparrow Coll}(z_{toc},\Omega,\Omega_0) = I_{bgd\mathbf{1}}^{\uparrow Coll}(z_{toc},\Omega,\Omega_0) + I_{bgd\mathbf{n}}^{\uparrow Coll}(z_{toc},\Omega,\Omega_0) \quad (3)$$

where

$$I_{bgd\mathbf{1}}^{\uparrow Coll}(z_{toc},\Omega,\Omega_0) = \frac{1}{\pi}\int_0^1\int_{2\pi}\int_0^1\int_{2\pi} \rho_{bgd}(z_{bgd},\Omega'',\Omega') I_{bgd}^{\downarrow Coll} \cdot (z_{bgd},\Omega',\Omega_0) \times T_{bgd}^{\uparrow Coll}(z_{toc},\Omega,\Omega'')\mu'\, d\Omega'\, d\Omega'' \quad \text{for } (\Omega' \neq \Omega_0 \text{ and } \Omega'' \neq \Omega) \quad (4)$$

Here $I_{bgd}^{\downarrow Coll}$ is the direct and diffuse downward radiation incident on the background and $T_{bgd}^{\uparrow Coll}$ is the total bidirectional transmission distribution function of the vegetation layer in direction Ω of the upwelling radiance field scattered once by the background in direction Ω''. $I_{bgd}^{\downarrow Coll}$ and $T_{bgd}^{\uparrow Coll}$ incorporate all contributions, including the directly transmitted radiation, due to the scattering of radiation in all downward and upward directions by the vegetation elements. By contrast, the ultimate term in (3), namely, $I_{bgd\mathbf{n}}^{\uparrow Coll}$ is a complex function of all structural and mainly spectral properties of both the vegetation layer and the underlying background. Since the background scattering properties are assumed to be spatially uniform, both (2) and (3) are expressed as functions of the same BRF function for the background, namely, $\rho_{bgd}(z_{bgd}, \Omega, \Omega_0)$.

[21] Through its mathematical formulation, the RPV model [*Rahman et al.*, 1993] splits a BRF field into its amplitude component and the associated angular field describing the anisotropy of the background; that is,

$$\rho_{bgd}(z_{bgd},\Omega,\Omega_0;\rho_0,\rho_c,\Theta,k) = \rho_0\,\breve{\rho}_{bgd}(z_{bgd},\Omega,\Omega_0;\rho_c,\Theta,k) \quad (5)$$

where ρ_0 and $\breve{\rho}_{bgd}(z_{bgd}, \Omega, \Omega_0; \rho_c, \Theta, k)$ describe the amplitude and the angular field of the background BRF, respectively. This latter quantity as well as the overall model performances are described elsewhere [*Engelsen et al.*, 1996; *Pinty et al.*, 2002; *Gobron and Lajas*, 2002]. Briefly the parameter k, entering a modified version of the Minnaert's function, controls the bowl/bell-shape patterns of the BRF fields, the parameter Θ establishes the degree of forward versus backward scattering, depending on its sign, following the Henyey-Greenstein formulation and the parameter ρ_c accounts for the hot spot effect especially significant in the exact backscattering direction. For all practical purposes, we will neglect this latter contribution in the forthcoming developments. The angular function of the RPV model, $\breve{\rho}_{bgd}(z_{bgd}, \Omega, \Omega_0; \Theta, k)$ is constant and equal to unity in the case of an isotropic background. This condition is fulfilled by setting simultaneously $k = 1$ in the modified Minnaert's function and $\Theta = 0$ in the Henyey-Greenstein function. In such a case, the ρ_0 factor is numerically identical to the bihemispherical albedo of the background.

[22] One major advantage of the RPV model is that the amplitude of the BRF appears as a factor to an angular function. Since the contributions to the upward radiance from all scattering events involving the background (as expressed through (2) and (3)) implies the multiplication of the downwelling radiance by the BRF of the background, it is very convenient to factor out the amplitude parameter, namely ρ_0, in these equations. Following this strategy, (1) can be rewritten as:

$$I_{coupled}^{\uparrow total}(z_{toc},\Omega,\Omega_0) = I_{veg}^{\uparrow Coll}(z_{toc},\Omega,\Omega_0;\mathbf{B},\mathbf{O},\mathbf{S},LAI_{scene}) + \rho_0\left[\breve{I}_{bgd}^{\uparrow UnColl}\left(z_{toc},\Omega,\Omega_0;\mathbf{B},\mathbf{S},.LAI_{scene},BRF_{bgd}^{shape}\right) + \breve{I}_{bgd}^{\uparrow Coll}(z_{toc},\Omega,\Omega_0;\mathbf{B},\mathbf{O},\mathbf{S},LAI_{scene},BRF_{bgd})\right] \quad (6)$$

with

$$\breve{I}_{bgd}^{\uparrow Coll}(z_{toc},\Omega,\Omega_0) = \breve{I}_{bgd\mathbf{1}}^{\uparrow Coll}\left(z_{toc},\Omega,\Omega_0;\mathbf{B},\mathbf{O},\mathbf{S},LAI_{scene},BRF_{bgd}^{shape}\right) + \breve{I}_{bgd\mathbf{n}}^{\uparrow Coll}(z_{toc},\Omega,\Omega_0;\mathbf{B},\mathbf{O},\mathbf{S},.LAI_{scene},BRF_{bgd}) \quad (7)$$

In that instance, radiance quantities noted $\breve{I}$ correspond to the shape of the angular fields (identified by symbol $\breve{}$) of the various contributions to the upward radiance at level z_{toc}. It is noteworthy that $\breve{I}_{bgd\mathbf{n}}^{\uparrow Coll}(z_{toc}, \Omega, \Omega_0; \mathbf{B}, \mathbf{O}, \mathbf{S}, LAI_{scene}, BRF_{bgd})$ is still a function of the amplitude of the BRF of the background, and not only of its BRF shape, due to the multiple interactions between the background and the canopy. Equations (6) and (7) can be written equivalently after multiplication by the factor $\pi/E_0\ \mu_0$ to transform radiances into BRFs or diffuse bidirectional transmission factors, as appropriate.

[23] A few critical remarks are in order at this point:

[24] 1. Equation (6) is equally valid for structurally homogeneous and heterogeneous vegetation canopy situations.

[25] 2. The mathematical developments yielding (6) are targeted to the vegetation canopy problem but they apply to any discrete medium, e.g., clouds and soil, in the limits of the assumptions required for defining the "radiatively independent volume."

[26] 3. The radiation transfer problem of a scattering/absorbing turbid layer, e.g., an atmospheric aerosol layer overlying an anisotropic soil, constitutes only a limit case of (6). Indeed, due to the absence of voids in the scattering/absorbing turbid layer that is made up of scatterers whose size tends to zero, the quantity $I_{bgd}^{\downarrow UnColl}(z_{toc}, \Omega, \Omega_0)$ becomes equivalent to the direct downwelling radiance attenuated exponentially along direction Ω_0, scattered by the background and directly transmitted exponentially through the turbid layer in direction Ω.

[27] 4. Equation (6) is quasi-linear with respect to the amplitude of the background BRF. The departure from linearity is induced by the second term in (7) featuring the contribution from multiple scattering between the background and the vegetation layer.

[28] 5. All terms in (6) except the second in (7) can be precomputed and stored in LUTs for both forward and inverse modeling purposes at a limited cost since the dependency of the contributing kernels with respect to the

amplitude of the background BRF has been factored out. In that instance and for a given set of attributes specified by **B**, **O**, **S**, LAI_{scene} and, BRF_{bgd}^{shape}, only a limited number of simulations by the full 3-D radiation transfer model are required for computing the first two terms in (6) for a range of Ω, Ω_0 values; indeed, the first and second term in (6) need only to be estimated on the basis of the "Black Background" and "Black Canopy" conditions, respectively.

[29] The contribution from the second term in (7) is still problematic in the perspective of performing a 3-D model inversion, due to its dependency on the amplitude of the background BRF, ρ_0. In order to avoid creating a very large number of LUTs for each and every background BRF conditions per scene, it is thus desirable to reformulate the second term in (7) such that its estimation becomes more computer efficient.

3.2. Azimuthal Average of the Diffuse Radiance Fields Scattered by the Background

[30] Given that the leaf scattering phase functions are rather smooth in the azimuthal plane, e.g., bi-Lambertian scattering phase function are generally adopted, it may be accurate enough to approximate the diffuse bidirectional transmission distribution functions by their azimuthal averages. The use of azimuthally averaged quantities for representing the multiply scattered contribution is known to be accurate within a 1.5% range in the limit case of turbid medium layer overlying an isotropic background [*Shultis and Myneni*, 1988; *Gobron et al.*, 1997b]. The implementation of this approximation allows us to rewrite (6) and (7) as follows in terms of BRF quantities:

$$\begin{aligned}\rho_{coupled}^{total}(z_{toc},\Omega,\Omega_0) = {} & \rho_{veg}^{Coll}(z_{toc},\Omega,\Omega_0;\mathbf{B},\mathbf{O},\mathbf{S},LAI_{scene}) \\ & + \rho_0\Big[\breve{\rho}_{bgd}^{UnColl}\Big(z_{toc},\Omega,\Omega_0;\mathbf{B},\mathbf{S},.LAI_{scene}, \\ & BRF_{bgd}^{shape}\Big) \\ & + \breve{\rho}_{bgd}^{Coll}\big(z_{toc},-\mu,\mu_0;\mathbf{B},\mathbf{O},\mathbf{S},LAI_{scene}, \\ & BRF_{bgd}\big)\Big] \end{aligned} \tag{8}$$

where

$$\begin{aligned}\breve{\rho}_{bgd}^{UnColl}(z_{toc},\Omega,\Omega_0) = {} & T_{bgd}^{\downarrow UnColl}\big(z_{bgd},\Omega_0\big)\breve{\rho}_{bgd}\big(z_{bgd},\Omega,\Omega_0\big)T_{bgd}^{\uparrow UnColl} \\ & (z_{toc},\Omega) \end{aligned} \tag{9}$$

$$T_{bgd}^{\downarrow UnColl}\big(z_{bgd},\Omega_0\big) = I_{bgd}^{\downarrow UnColl}\big(z_{bgd},\Omega_0\big)/E_0\,\delta(\mu_0-\mu)\,\delta(\phi_0-\phi) \tag{10}$$

and

$$\begin{aligned}\breve{\rho}_{bgd}^{Coll}(z_{toc},-\mu,\mu_0) = {} & \breve{\rho}_{bgd\mathbf{1}}^{Coll}\Big(z_{toc},-\mu,\mu_0;\mathbf{B},\mathbf{O},\mathbf{S},LAI_{scene},BRF_{bgd}^{shape}\Big) \\ & + \breve{\rho}_{bgd\mathbf{n}}^{Coll}(z_{toc},-\mu,\mu_0;\mathbf{B},\mathbf{O},\mathbf{S},LAI_{scene},BRF_{bgd}) \end{aligned} \tag{11}$$

where $\breve{\rho}_{bgd\mathbf{1}}^{Coll}(z_{toc}, -\mu, \mu_0)$ represents the angular field of the BRF contribution reaching the top of the layer involving either or both the diffuse downwelling and upwelling radiation scattered using the azimuthally averaged background BRF model. In (11) and subsequent equations, the functions and factors applied to characterize the origin and direction of the radiation are identified by negative (positive) values of the cosine of the zenith angles (μ) for upward (downward) traveling directions.

3.3. Homogeneous Plane-Parallel Turbid Medium Based Approximations

[31] To further limit the computational cost of the algorithm, including the size of the LUTs to be manipulated, additional developments, that translate into simplifications of the structure of the vegetation layer, have to be proposed for some of the less contributing terms in (8). In that instance, the calculation of the BRFs involving the joint contributions from both the background and the diffuse transmission distribution functions in the vegetation layer, that is, $\breve{\rho}_{bgd\mathbf{1}}^{Coll}(z_{toc}, -\mu, \mu_0)$ and $\breve{\rho}_{bgd\mathbf{n}}^{Coll}(z_{toc}, -\mu, \mu_0)$ are good candidates since these quantities are less likely to be very sensitive to the effects induced by the 3-D distribution of the scattering centers prevailing inside the "radiatively independent volume" of vegetation. Following this approach, it sounds attractive to approximate the two contributions in (11) in the limit of the equivalent plane-parallel homogeneous turbid medium layer condition. Such a radiative equivalence is, however, valid only to the extent that the effective values of the state variables entering the plane-parallel homogeneous (1-D) radiation transfer model are known. The radiatively effective values for LAI and leaf reflectance and transmittance factors (including the non-explicit contributions due to the stems) must be such that the equivalent plane-parallel homogeneous model delivers bidirectional reflectance factors or, at least, reflected radiant fluxes, corresponding to the contribution from $\breve{\rho}_{bgd}^{Coll}(z_{toc}, -\mu, \mu_0)$ that are ideally undiscernible from those produced by the 3-D radiation transfer model.

[32] Prior to addressing this crucial aspect, which is intimately linked to the 1-D based approach (see section 3.3.2), it is first required to establish an accurate parameterization of the radiation transfer regime into the equivalent turbid vegetation that enables, at best, the desired decoupling between the vegetation layer and its lower boundary condition, namely, the amplitude of the background BRF. The next section introduces such a parameterization which follows the strategy originally proposed for the MISR instrument to retrieve the aerosol load over dark surfaces [*Martonchik et al.*, 1998] and further extended to any surface type to jointly estimate the surface albedo and the aerosol load from geostationary satellite data [*Pinty et al.*, 2000a].

3.3.1. Parameterization of the Equivalent Turbid Medium Layer

[33] With some adaptation to the vegetation problem of the approach proposed by *Martonchik et al.* [1998] and *Pinty et al.* [2000a], the contribution from $\breve{\rho}_{bgd\mathbf{n}}^{Coll}(z_{toc}, -\mu, \mu_0)$, in the case of a plane-parallel homogeneous turbid medium layer, can be approximated by

$$\begin{aligned}\breve{\rho}_{bgd\mathbf{n}}^{\|Coll}(z_{toc},-\mu,\mu_0) \approx {} & \pi\, S_{bgd\mathbf{n}}^{\|Coll}\big(z_{bgd},\mu_0\big) \\ & \cdot\Big[\exp\Big(-\widetilde{LAI}/2\,|\mu|\Big)\breve{A}(-\mu)+a(-\mu)\Big] \end{aligned} \tag{12}$$

where $\widetilde{LAI}$ corresponds to the effective leaf area index of the plane-parallel turbid medium layer (identified by the symbol $\|$), assumed to be made of nonoriented uniformly distributed point-like scatterers. The factor 1/2 intervening in the argument of the exponential is due to the use of a uniform leaf angle distribution function [e.g., *Ross*, 1981]. The use of this latter function is not mandatory, but it simplifies the developments further and is believed to be appropriate for most applications in inverse mode at the spatial resolution of the "radiatively independent volume."

[34] The term $S^{\|Coll}_{bgd\mathbf{n}}(z_{bgd}, \mu_0)$ in (12) represents the source term at the background level due to multiple scattering between the background and the vegetation layer in its turbid representation. It can be approximated by

$$S^{\|Coll}_{bgd\mathbf{n}}(z_{bgd}, \mu_0) \approx \frac{\breve{A}(\mu_0)\overline{\rho}_{veg}}{1 - \rho_0\,\alpha_0\,\overline{\rho}_{veg}}\,\rho_0 \cdot \frac{\left[\exp\left(-\widetilde{LAI}/2\,\mu_0\right) + \overline{T}^{\|Coll}_{bgd\mathbf{1}}(z_{bgd}, \mu_0)\right]}{\pi} \tag{13}$$

where

$$\alpha_0 = 4\int_0^1\int_0^1 r_0(-\mu, \mu')\mu'\,d\mu'\,\mu\,d\mu \tag{14}$$

$$\overline{\rho}_{veg} = \frac{1}{\pi^2}\int_0^1\int_0^{2\pi}\int_0^1\int_0^{2\pi} \rho^{\|Coll}_{veg}(z_{bot}, \mu, -\mu', \phi' - \phi) \cdot \mu'\,d\mu'\,d\phi'\,\mu\,d\mu\,d\phi \tag{15}$$

$$\breve{A}(-\mu) = 2\int_0^1 r_0(-\mu, \mu')\,\mu'\,d\mu' \tag{16}$$

and

$$a(-\mu) = \int_0^1 T_0(-\mu, -\mu')\breve{A}(-\mu')\,\mu'\,d\mu' \tag{17}$$

$\overline{\rho}_{veg}$ is the bihemispherical albedo of the turbid vegetation layer over a black background. Since the vertical profile in leaf area density is assumed constant in the turbid layer, the quantity $\rho^{\|Coll}_{veg}(z_{bot}, \mu, -\mu', \phi' - \phi)$ is equal to the BRF of the equivalent plane-parallel turbid vegetation layer when illuminated from below.

[35] The bracketed terms in (13) correspond to the contribution due to the total (direct + diffuse) transmission of the vegetation layer for a black background condition. The direct component is equal to $\exp(-\widetilde{LAI}/2\ \mu_0)$ and the directional hemispherical transmission function associated with the downward flux diffusively transmitted at level z_{bgd}, $\overline{T}^{\|Coll}_{bgd\mathbf{1}}(z_{bgd}, \mu_0)$, is given by

$$\overline{T}^{\|Coll}_{bgd\mathbf{1}}(z_{bgd}, \mu_0) = \int_0^1 T_0(\mu, \mu_0)\,\mu\,d\mu \tag{18}$$

[36] The functions r_0 and T_0 are the azimuthally averaged angular fields of the background BRF and diffuse bidirectional transmission distribution function of the turbid vegetation layer, respectively:

$$T_0(\mu, \mu_0) = 2\,I^{\|Coll}_{bgd\mathbf{1}}(z_{bgd}, \mu, \mu_0)/E_0\,\mu_0 \tag{19}$$

and

$$r_0(-\mu, \mu') = \frac{1}{2\pi}\int_0^{2\pi} \breve{\rho}_{bgd}(z_{bgd}, -\mu, \mu', \phi - \phi')d\phi' \tag{20}$$

Incidentally, $\breve{A}(-\mu)$ represents the angular shape of the directional hemispherical reflectance of the background. The latter quantity is equal to the product $\rho_0\,\breve{A}(-\mu)$ and thus, according to (17), independent from the downwelling radiance field scattered in the vegetation layer. By contrast, the product $\rho_0\,\alpha_0$ where α_0 is defined by (14) corresponds to the bihemispherical reflectance of the anisotropic background assuming an isotropic angular distribution of the downwelling radiance field scattered in the vegetation layer.

[37] For a given ρ_0 value, (12) can thus be estimated by precomputing, on the basis of the effective values for the input state variables, the values of the functions $\breve{A}(-\mu)$, $a(-\mu)$, $\overline{T}^{\|Coll}_{bgd\mathbf{1}}(z_{bgd}, \mu_0)$, $\overline{\rho}_{veg}$ and α_0.

[38] The plane-parallel homogeneous turbid medium approach can as well be used further to approximate the first contributing term in (11), $\breve{\rho}^{Coll}_{bgd\mathbf{1}}$. This contribution can be expressed as follows:

$$\breve{\rho}^{\|Coll}_{bgd\mathbf{1}}, \mu_0) \approx \exp\left(-\widetilde{LAI}/2\,|\mu|\right) f_0(-\mu, \mu_0) + \exp\left(-\widetilde{LAI}/2\,\mu_0\right) g_0(-\mu, \mu_0) + h_0(-\mu, \mu_0) \tag{21}$$

where

$$\begin{aligned} f_0(-\mu, \mu_0) &= \int_0^1 T_0(\mu', \mu_0) r_0(-\mu, \mu')\,\mu'\,d\mu' \\ g_0(-\mu, \mu_0) &= \int_0^1 T_0(-\mu, -\mu')\,r_0(-\mu', \mu_0)\,\mu'\,d\mu' \\ h_0(-\mu, \mu_0) &= \int_0^1 T_0(-\mu, -\mu') f_0(-\mu', \mu_0)\,\mu'\,d\mu' \end{aligned} \tag{22}$$

[39] In (21), and after multiplication by ρ_0, the first term represents the diffuse incoming radiation scattered by the background using the azimuthally averaged BRF model and reaching the top of the turbid vegetation layer after attenuation by the transmission distribution function for direct radiation. The second term represents the direct incoming radiation scattered by the background using the azimuthally averaged BRF model and reaching the top of the turbid vegetation layer after attenuation by the transmission distribution function for upward diffuse radiation. The third term represents the diffuse incoming radiation scattered by the background using the azimuthally averaged BRF model and then attenuated in direction Ω by the bidirectional transmission factor for upward diffuse radiation.

[40] This mathematical development assumes that the upward and downward diffuse bidirectional transmission distribution functions are reciprocal in the turbid vegetation layer that is, for instance, $T_0(\mu, \mu') = T_0(-\mu', -\mu)$. This assumption is valid since, in its turbid representation, the

vegetation layer is vertically homogeneous. Note that the functions f_0, g_0 and h_0 could be written differently depending on the adopted sets of reciprocal relationships.

[41] This mathematical development was shown to be very accurate in the case of a plane-parallel scattering atmosphere when expanding the diffuse bidirectional transmission distribution function as cosine Fourier series limited to the first two terms [*Martonchik et al.*, 2002]. Several tests were conducted to evaluate the performance of the parameterization proposed to estimate (12) and (21) in the limit case of a plane-parallel homogeneous turbid vegetation layer. These tests were conducted using the 1/2 Discrete model [*Gobron et al.*, 1997b] whose performance for simulating structurally homogeneous vegetation has been assessed in the context of the Radiation Transfer Model Intercomparison (RAMI) exercise [*Pinty et al.*, 2004]. This model implements a discrete ordinate method for the estimation of the multiple scattering processes. We found excellent agreement (within 1% range relative) between the 1/2 Discrete based simulations of (11) and those obtained using (12) and (21), even for extreme full conservative conditions and anisotropic scattering functions similar to those labeled as "purist corner" in RAMI [*Pinty et al.*, 2001].

[42] In practice, this plane-parallel turbid medium assumption thus allows us to approximate the contribution due to the term $\breve{\rho}^{Coll}_{bgd\mathbf{1}}(z_{toc}, -\mu, \mu_0)$ by simply precomputing and storing the values of the functions $f_0(-\mu, \mu_0)$, $g_0(-\mu, \mu_0)$ and, $h_0(-\mu, \mu_0)$. Under conditions where both the use of azimuthally averaged quantities and the plane-parallel homogeneous turbid medium approximation are found acceptable, (8) is thus finally approximated by

$$\begin{aligned}\rho^{total}_{coupled}(z_{toc}, \Omega, \Omega_0) \approx \rho^{Coll}_{veg}(z_{toc}, \Omega, \Omega_0; \mathbf{B}, \mathbf{O}, \mathbf{S}, LAI_{scene}) \\ + \rho_0 \Big[\breve{\rho}^{UnColl}_{bgd}(z_{toc}, \Omega, \Omega_0; \mathbf{B}, \mathbf{S}, LAI_{scene}, k, \Theta) \\ + \breve{\rho}^{\|Coll}_{bgd}\left(z_{toc}, -\mu, \mu_0; \mathbf{B}, \tilde{\mathbf{O}}, \widetilde{LAI}_{scene}, k, \Theta, \rho_0\right)\Big]\end{aligned} \tag{23}$$

with

$$\begin{aligned}\breve{\rho}^{\|Coll}_{bgd}\left(z_{toc}, -\mu, \mu_0; \mathbf{B}, \tilde{\mathbf{O}}, \mathbf{S}, \widetilde{LAI}_{scene}, k, \Theta, \rho_0\right) \\ = + \breve{\rho}^{\|Coll}_{bgd\mathbf{1}}\left(z_{toc}, -\mu, \mu_0; \mathbf{B}, \tilde{\mathbf{O}}, \mathbf{S}, \widetilde{LAI}_{scene}, k, \Theta\right) \\ + \breve{\rho}^{\|Coll}_{bgd\mathbf{n}}\left(z_{toc}, -\mu, \mu_0; \mathbf{B}, \tilde{\mathbf{O}}, \mathbf{S}, \widetilde{LAI}_{scene}, k, \Theta, \rho_0\right)\end{aligned} \tag{24}$$

where $\tilde{\mathbf{O}}$ features the effective spectral values to be allocated to the scattering centers present in the equivalent plane-parallel homogeneous turbid medium vegetation volume.

3.3.2. Estimate of the Effective Radiative Quantities

[43] In order for the plane-parallel homogeneous turbid medium (1-D) radiation transfer model to generate radiance fields that are equivalent to the 3-D model, it is necessary to evaluate first the effective values of the state variables entering the 1-D model. The effectiveness of using equivalent plane-parallel models for mimicking the radiance fields emerging on both sides of an absorbing/scattering layer has long been recognized in various geophysical domains including cloud physics [e.g., *Cahalan et al.*, 1994; *Szczap et al.*, 2000; *Cairns et al.*, 2000; *Petty*, 2002] where there is a strong motivation to represent efficiently the effects due to cloud spatial heterogeneities at scales corresponding to the grid cells of atmospheric models. In most cloud-driven applications, this approach is adopted to represent the total BRFs and bidirectional transmission distribution functions emerging from the top and bottom sides, respectively, of a heterogeneous system. In the present study, we propose to limit the use of this approach for estimating the less contributing term in (8) only, that is, the term due to multiple scattering between the vegetation elements and the background surface.

[44] This task can be achieved using various approaches depending on the context and the physical complexity of the heterogeneous system to deal with. In the present study we propose to follow a heuristic approach taking advantage of the accurate Monte-Carlo ray tracing simulations for the first two terms in (8).

[45] First, unlike clouds and other atmospheric systems, the extinction coefficient of a vegetation canopy layer, that is, the leaf area density of that layer weighted by the leaf angle distribution function, is wavelength-independent. We can thus take advantage of this fact by separating the estimate of the effective LAI value, $\widetilde{LAI}$, from those properties pertaining to the spectrally dependent variables, namely, the leaf reflectance $\tilde{r}_l$ and leaf transmittance $\tilde{t}_l$. This specific vegetation characteristic translates into a much simpler situation than the cloud problem since, for instance, the effective values of the optical thickness of the cloud layer, the particle single-scattering albedo and phase functions are all wavelength-dependent.

[46] Second, the mathematical developments proposed in section (3) separate the so-called "Black Background" and "Black Canopy" contributions from the rest. Since the direct transmission distribution functions controlling the "Black Canopy" contribution follows the classical Beer's law exponential decay in the limit case of a turbid medium, the effective LAI value of the "radiatively independent volume" should logically satisfy the following relationship:

$$\widetilde{LAI}(\mu_0) = -2.0\,\mu_0\,\log\left[T^{\downarrow UnColl}_{bgd}(z_{bgd}, \mu_0)\right] \tag{25}$$

The presence of a hierarchy of gaps in the vegetation canopy implies that $\widetilde{LAI}(\mu_0)$ is lower than LAI_{scene} deduced from the volume weighted average. Depending on the structure of the scene, one should expect that this reduction gets, however, smaller for increasing Sun zenith angles.

[47] Third, the estimate of the leaf reflectance $\tilde{r}_l$ and leaf transmittance $\tilde{t}_l$ effective values must be achieved with no contamination by the lower boundary condition, that is, the background surface properties. It thus sounds logical to estimate these quantities on the basis of the reflected and diffusely transmitted radiant fluxes corresponding to the "Black Background" contribution. The joint use of both the upward and downward fluxes ensures assessing the correct estimate of $\tilde{r}_l$ and $\tilde{t}_l$ since their sum and ratio express the scattering efficiency and preferred scattering direction, respectively. The estimate of $\tilde{r}_l$ and $\tilde{t}_l$ can thus be achieved simply by inverting the 1-D turbid model, in a version implementing the effective LAI of the scene, against the

Table 1. Variables Defining the Structurally Heterogeneous Scenes

Variable Identification	Values (Units)
Mean Leaf Area Index of the scene	1.24[a], 2.0[b] and 4.82[c] (m^2/m^2)
Mean Leaf Area Index of a tree crown	6.02[a], 6.49[b] and 2.77[c] (m^2/m^2)
Gap fraction of the scene	0.83[a], 0.69[b] and 0.25[c]
Tree density	53[a], 142[b] and 4718[c] (trees/hectare)
Mean tree height	23.99[a], 24.49[b] and 9.92[c] (m)
Mean tree crown length	7.59[a], 7.09[b] and 7.57[c] (m)
Spatial distribution of tree locations	Poisson distribution
Scatterer shape	disc of negligible thickness
Scatterer radius	0.05 (m)
Scatterer normal distribution in tree crown	uniform

[a]Sparse vegetation condition.
[b]Medium vegetation condition.
[c]Dense vegetation condition.

Monte-Carlo ray tracing simulations of this contribution. Hence the search of the optimal $\widetilde{r_l}$ and $\widetilde{t_l}$ values boils down to minimizing jointly the following metrics, up to the accuracy level of the models,

$$\sum_{\mu_0} \left| \overline{R}_{veg}^{Coll}\left(z_{toc}, \mu_0; \mathbf{B}, \mathbf{O}, \mathbf{S}, LAI_{scene}\right) - \overline{R}_{veg}^{\|Coll}\left(z_{toc}, \mu_0; \widetilde{r_l}, \widetilde{t_l}, \widetilde{LAI}(\mu_0)\right) \right| \tag{26}$$

and

$$\sum_{\mu_0} \left| \overline{T}_{bgd\mathbf{1}}^{Coll}\left(z_{bgd}, \mu_0; \mathbf{B}, \mathbf{O}, \mathbf{S}, LAI_{scene}\right) - \overline{T}_{bgd\mathbf{1}}^{\|Coll}\left(z_{bgd}, \mu_0; \widetilde{r_l}, \widetilde{t_l}, \widetilde{LAI}(\mu_0)\right) \right| \tag{27}$$

where $\overline{R}_{veg}^{Coll}$ ($\overline{T}_{bgd\mathbf{1}}^{Coll}$) and $\overline{R}_{veg}^{\|Coll}$ ($\overline{T}_{bgd\mathbf{1}}^{\|Coll}$) denote the directional hemispherical reflectance (diffuse transmission function) simulated with the Monte-Carlo ray tracing model and the equivalent plane-parallel turbid medium model, respectively, for the "Black background" contributions. Equations (26) and (27) impose that the reflected and transmitted radiant fluxes, two hemispherical quantities, resulting from the "Black Background" contribution remain conserved when inverting the equivalent plane-parallel 1-D turbid model. The joint use of two hemispherical quantities permits us decoupling the individual effects of $\widetilde{r_l}$ and $\widetilde{t_l}$ and ensuring that the absorbed flux by the vegetation layer is conserved as well inside the "radiatively independent volume."

[48] Since the effective LAI value is changing with μ_0, the effective leaf reflectance and transmittance values, and more specifically their sum, exhibit some dependency with respect to the Sun zenith angle condition. However, the latter was found to be weak enough, and mostly within the uncertainty range associated with their estimates, such that it can be neglected for the purpose of the current application, that is, the estimate of (24).

3.3.3. Performance of the 1-D Turbid Medium Approximation

[49] The two main remaining issues at this point are to evaluate (1) the relative contribution of the third term in equation (8) with respect to the total BRF signal and (2) whether equation (24) constitutes an appropriate estimate of equation (7) for most applications.

[50] The radiation transfer regimes of a series of 3-D scenes were calculated using the Raytran ray tracing Monte-Carlo model [*Govaerts and Verstraete*, 1998] and the three separate contributions, namely, those due to the "Black Background," the "Black Canopy," and the multiple scattering between the background and the canopy, respectively, were estimated separately as proposed in (8). All simulations performed in the context of this paper implement an isotropic scattering law for the background and a bi-Lambertian law for the leaf reflectance and transmittance. They also all correspond to a spatial resolution of 250 m, in order to mimic the measurements collected by various multispectral, multiangular medium resolution space sensors. Tables 1 and 2 summarize the geophysical scenarios that were selected in order to span a range of conditions regarding the vegetation density and spatial distribution, as well as the background radiative properties. These simulated conditions were then further used to provide some answers to the two points mentioned considering both typical and extreme scenarios. The relative contributions of each component in (6) were thus analyzed for typical canopy and background conditions measured in the red and the near-infrared spectral domain as well as for a very bright background mimicking snow cover conditions in the near-infrared domain only.

[51] The various panels in Figure 1 illustrate, on the basis of the 3-D Raytran model simulations, the relative contributions to the total BRF, $\rho_{coupled}^{total}$, of the three kernels identified in (6) and (8), namely, the "Black Background" ρ_{veg}^{Coll}, the "Black Canopy" ρ_{bgd}^{UnColl}, and the coupled Canopy-Background scattering ρ_{bgd}^{Coll}. The plots are shown as a function of the viewing zenith angle in the cross plane, that is, the plane orthogonal to the principal plane defined by the local normal and the Ω_0 vector, for two Sun zenith angle conditions, 30° and 60°, and for the three geophysical scenarios described in Tables 1 and 2. As anticipated, the "Black Background" and "Black Canopy" contributions are contrasted via their bowl versus bell shapes [*Pinty et al.*, 2002]. It can readily be seen that the approximation of ρ_{bgd}^{Coll} will concern at most 15 to 35% of the total signal in the snow cover scenario and 5 to 15% (less than 5%) in the typical near-infrared (red) scenario. Indeed, the relative contribution of this term is mainly controlled by the single scattering albedo of the leaves and the background brightness. This contribution is therefore very low in the red spectral domain under typical conditions and becomes more significant in the near-infrared part especially with a bright background condition.

[52] The various geophysical scenarios were all analyzed to retrieve the values of the effective variables following the procedure described in section (3.3.2). Table 3 summarizes

Table 2. Variables Defining the Spectral Leaf and Soil Properties of the Structurally Heterogeneous Scenes

Variable Identification	Red Values	Near-Infrared Values
Leaf scatterer reflectance[a]	0.018	0.486
Leaf scatterer transmittance[a]	0.021	0.462
Trunk reflectance[b]	0.294	0.591
Soil reflectance[b]	0.173[c]	0.206[c] and 0.814[d]

[a]Using a bi-Lambertian scattering law.
[b]Using a Lambertian scattering law.
[c]Typical scenario conditions.
[d]Snow cover conditions simulated in the near-infrared.

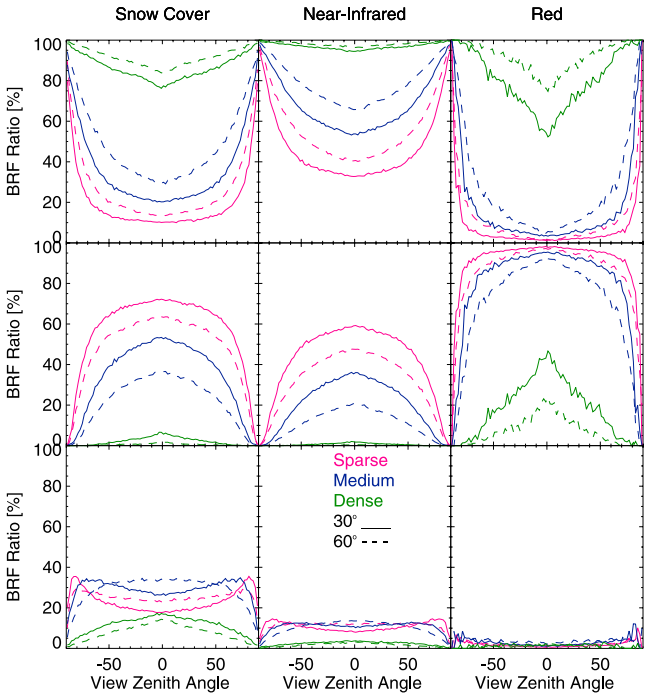

Figure 1. Relative contributions to the total BRF, $\rho_{coupled}^{total}$, of the "Black Background," ρ_{veg}^{Coll}, the "Black Canopy" ρ_{bgd}^{UnColl} and the coupled Canopy-Background scattering ρ_{bgd}^{Coll}. The plots are shown as a function of the viewing zenith angle in the cross plane, that is, the plane orthogonal to the principal plane defined by the local normal and the Ω_0 vector, for two Sun zenith angle conditions, 30° and 60°, and for the three geophysical scenarios described in Tables 1 and 2.

the results of the estimate of the effective LAI values, $LAI(\mu_0)$, as deduced from (25) for each set of structural and illumination conditions. As anticipated, the effective LAI value is much lower than the domain-averaged LAI values of the scenes and the LAI reduction factor lies in between approximately 0.3 for the low density and 0.8 for the large density conditions we adopted here.

[53] This reduction in LAI is accompanied by substantial changes in the scatterer reflectance and transmittance values for the typical near-infrared scenarios. Indeed, the effective scatterer reflectance and transmittance values and especially their sum are found to be smaller by approximately 12% (for the dense canopy) to 18% (for the sparse canopy) than the corresponding actual values implemented in the 3-D simulations. Further studies need to be conducted in order to assess the consequences of this finding but, as such, it indicates that, for the same reflected radiant flux, the 3-D structurally heterogeneous vegetation absorbs more than its equivalent 1-D turbid medium representation in a "radiatively independent volume." At this same wavelength, the correct estimation of the diffusely transmitted fluxes imposes the introduction of a significant anisotropy in the scattered fields. Indeed although the actual ratio of the scatterer reflectance to transmittance values is close to unity for all 3-D scenarios, the ratios of the effective values indicate strong predominant backward scattering regimes in the 1-D turbid medium representation. The actual diffuse downward transmitted fluxes generated by the 3-D Raytran model, are indeed smaller than those modeled using the equivalent 1-D turbid medium representation when conserving the scatterer reflectance to transmittance ratio. Therefore the correct partitioning between the upward and downward fluxes requires increasing significantly this ratio as reported in Table 4. The decrease in the downward diffuse fluxes can be interpreted as a consequence of the enhanced absorption efficiency in the 3-D structurally heterogeneous scenarios when compared to the 1-D turbid medium representation. We may, indeed, hypothesize that, in the latter case, more radiation is lost due to absorption of radiation multiply scattered in the horizontal directions, e.g., photon trapping in between the trees. The proper interpretation of this phenomenon requires further detailed studies of the local radiation budgets at high spatial resolutions inside the "radiatively independent volume."

[54] It is noticeable that the equivalent 1-D turbid medium is able to simulate within a few percent relative accuracy the reflected, transmitted and absorbed radiant fluxes provided the optimal effective values for the three state variables are used. This finding thus illustrates that, at least in the case of a black background, it is possible to simulate accurately the three main radiant fluxes characterizing the radiative state of a 3-D heterogeneous environment using a plane-parallel model. When such a situation occurs, the values of the state variables entering the plane-parallel model must differ, sometimes significantly, from the corresponding domain-averaged values adopted in the 3-D heterogeneous scenario.

[55] In the red spectral domain, the radiation transfer regime is largely controlled by single scattering processes due to the high absorption efficiency by green leaves at this wavelength. The remaining amount of radiation available for multiple interactions between the vegetation layer and the background being thus extremely small (see the bottom right panel in Figure 1), distinguishing between a simple average (between leaf and woody element properties) and the effective values is of little concern in this case. We noticed, however, a systematic increase in the effective values of the single scattering albedo with respect to the actual values adopted for the leaves (see Table 5). This increase may simply illustrate the additional but complex role of the stems and trunks whose reflectance values exceed those of the strongly absorbing leaves. In such conditions, the 1-D turbid medium representation requires to take on values for the effective optical properties that are basically smoothing the effects due to the foliage and woody elements embedded in the vegetation layer. Note that no attempt was made here to separate the woody from the leaf elements in estimating these effective values.

Table 3. Effective Values of the Leaf Area Index Entering the Equivalent 1-D Turbid Model

Variable Identification	Scenario	30°	60°
Mean Leaf Area Index of the scene, m^2/m^2	sparse	0.442	0.479
	medium	0.896	1.061
	dense	3.677	3.667
Reduction factor of the actual Leaf Area Index of the scene	sparse	0.356	0.386
	medium	0.448	0.530
	dense	0.763	0.761

Table 4. Effective Values of Optical Properties in the Near-Infrared Domain

Variable Identification	Scenario	Values[a]
Scatterer reflectance $\widetilde{r}_l$	sparse	0.642
	medium	0.680
	dense	0.728
Scatterer transmittance $\widetilde{t}_l$	sparse	0.138
	medium	0.118
	dense	0.102
Single scattering albedo $(\widetilde{r}_l + \widetilde{t}_l)$	sparse	0.780
	medium	0.798
	dense	0.830
Ratio between the equivalent and actual single scattering albedo[b]	sparse	0.823
	medium	0.843
	dense	0.876
Preferred scattering direction $(\widetilde{r}_l/\widetilde{t}_l)$[c]	sparse	4.65
	medium	5.76
	dense	7.14

[a]Using the Discrete model of *Gobron et al.* [1997b] to minimize (26) and (27).
[b]With respect to the leaf optical properties only.
[c]Values > 1.0 (<1.0) indicate predominant backward (forward) scattering direction.

[56] The retrieved effective values were further used to estimate the radiative contribution approximated by $\rho_{bgd}^{\|Coll}(z_{toc}, -\mu, \mu_0; \mathbf{B}, \widetilde{\mathbf{O}}, \widetilde{LAI}_{scene}, k, \Theta, \rho_0)$ as expressed by (24). Figure 2 displays, for this coupled Canopy-Background contribution in the near-infrared domain, the relative differences between simulations performed using the 3-D Raytran model for the actual geophysical scenarios and the equivalent 1-D turbid medium model implementing the effective values for the LAI and the leaf scatterer reflectance and transmittance in a plane-parallel approximation. The results of this intercomparison are shown here for viewing angles varying between 0° and 80°, for two Sun zenith angle conditions, namely 30° and 60°, and for the three geophysical scenarios described in Tables 1 and 2. It can be seen that the proposed parameterization, when applied with the appropriate effective values for the state variables, generates values that are very close to the 3-D ray tracing Monte-Carlo model. It is worthwhile remembering that this agreement does not result from a fitting of the 3-D explicit solution, but uses the effective variable values in direct mode to reconstruct this contribution. Thus the 3-D model is only required to estimate the "Black Blackground" and the "Black Canopy" angular contributions, while the 1-D model is used to estimate all other terms.

Table 5. Effective Values of Optical Properties in the Red Domain

Variable Identification	Scenario	Values[a]
Scatterer reflectance $\widetilde{r}_l$	sparse	0.021
	medium	0.017
	dense	0.015
Scatterer transmittance $\widetilde{t}_l$	sparse	0.025
	medium	0.027
	dense	0.023
Single scattering albedo $(\widetilde{r}_l + \widetilde{t}_l)$	sparse	0.046
	medium	0.044
	dense	0.038

[a]Using the 1/2 Discrete model of *Gobron et al.* [1997b] to minimize (26) and (27).

[57] Figures 3 and 4 illustrate that this parameterization permits us describing quite accurately the angular patterns corresponding to the individual coupled Canopy-Background contributions noted $\breve{\rho}_{bgd\mathbf{1}}^{Coll}(z_{toc}, -\mu, \mu_0)$ and $\breve{\rho}_{bgd\mathbf{n}}^{Coll}(z_{toc}, -\mu, \mu_0)$, respectively, for both typical and snow cover background scenarios in the near-infrared domain. These plots correspond to simulation results in the cross plane and for two Sun zenith angles. Quite similar patterns are exhibited in the principal plane (not shown). These results demonstrate that the parameterization captures most of the physics controlling the radiation transfer regimes associated with this contribution.

4. Inversion Method

[58] As explained already, various degrees of approximation can be adopted for the evaluation of $\breve{\rho}_{bgd}^{Coll}(z_{toc}, \Omega, \Omega_0)$ and (24) corresponds to the solution based upon the plane-parallel turbid medium assumptions proposed here. In short, (23) merges simulation results from 3-D and 1-D radiation transfer models. For any predefined vegetation type and associated LAI_{scene} value, the 3-D model is used to estimate accurately the angular field of the collided "Black Blackground" and the uncollided "Black Canopy" contributions, respectively. The 1-D model, designed for estimating the radiation transfer solutions in the case of structurally homogenous vegetation layers, is used for assessing the

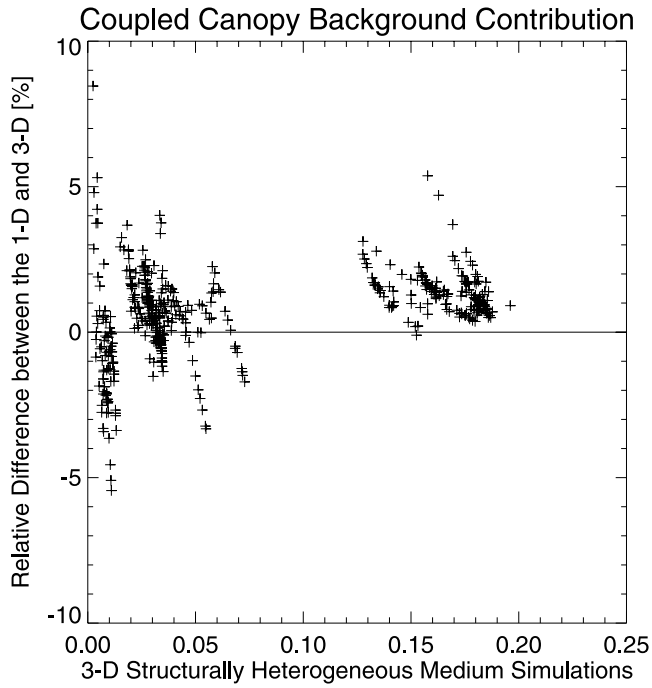

Figure 2. Relative differences (in percent) between BRF simulation results of the coupled Canopy-Background contribution delivered by the 3-D Raytran model and the equivalent 1-D turbid medium model implementing the effective values for the LAI and the leaf scatterer reflectance and transmittance in a plane-parallel approximation. The results of this intercomparison are shown here for viewing angles varying between 0° and 80°, for two Sun zenith angle conditions, namely 30° and 60°, and for the three geophysical scenarios described in Tables 1 and 2.

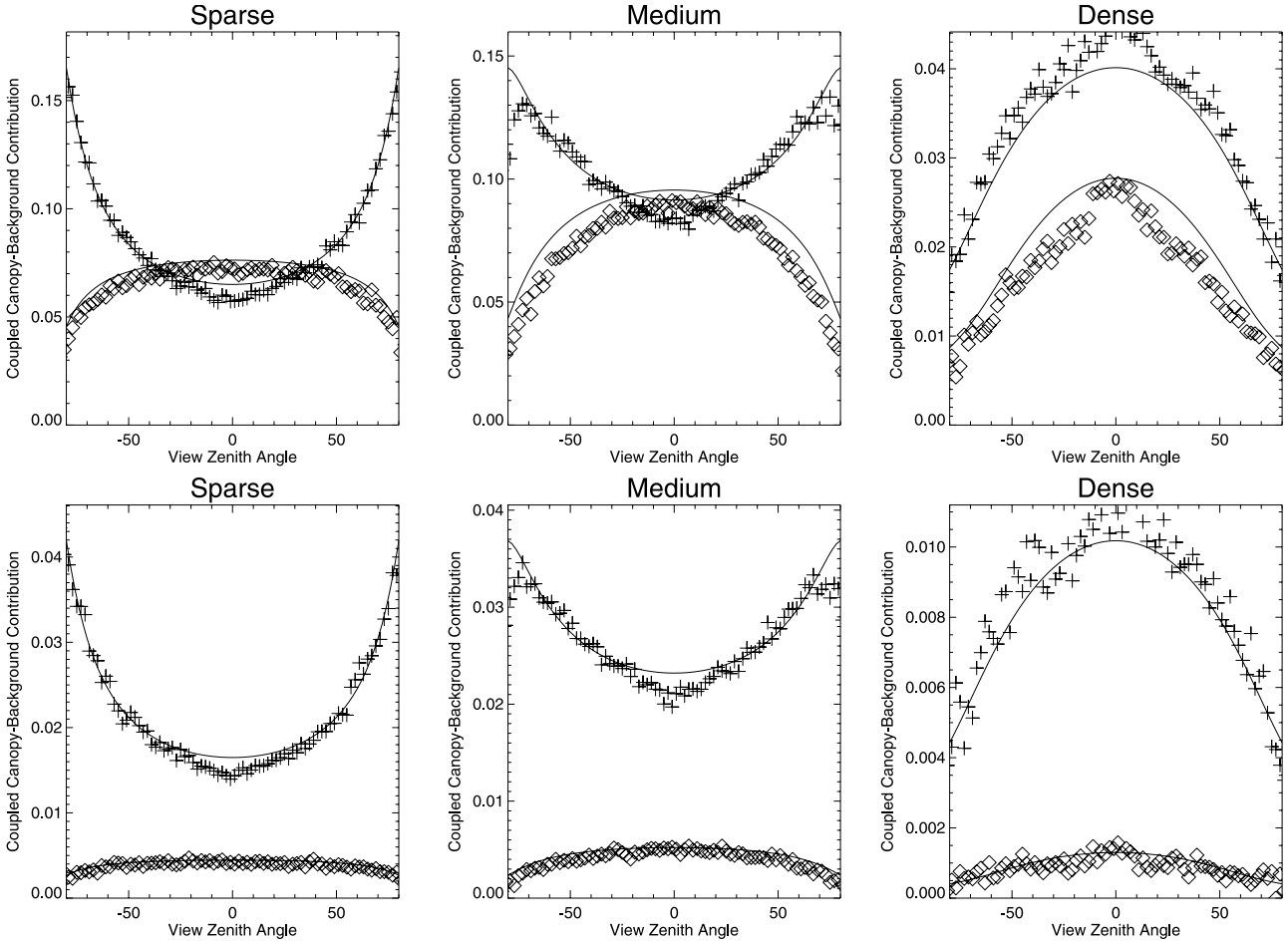

Figure 3. Intercomparison between BRF simulation results of the individual coupled Canopy-Background contributions, in the near-infrared domain, delivered by the equivalent 1-D turbid medium model (solid lines) and the 3-D Raytran model: crosses (diamonds) correspond to the contribution involving only one (more than one) scattering by the background, $\rho_{bgd\mathbf{1}}^{Coll}(z_{toc}, \Omega, \Omega_0)$ ($\rho_{bgd\mathbf{n}}^{Coll}(z_{toc}, \Omega, \Omega_0)$) in (7). The top (bottom) three panels are for the snow cover (typical soil) conditions. The plots are shown in the cross plane for a Sun zenith angle of 30° and for the three geophysical scenarios described in Table 1.

values of the following parameters and functions: $\check{A}(-\mu)$, $a(-\mu)$, $\overline{T}_{bgd\mathbf{1}}^{\|Coll}(z_{bgd}, \mu_0)$, $\overline{\rho}_{veg}$, α_0, $f_0(-\mu, \mu_0)$, $g_0(-\mu_0, \mu)$ and, $h_0(-\mu, \mu_0)$ on the basis of the effective values obtained for the 1-D model state variables. Once these functions and parameters values are known, (23) can be adopted to estimate simply for any background reflectance properties the BRF values emerging at the top of a structurally heterogeneous vegetation layer.

[59] Irrespective of the 3-D and 1-D models chosen to represent the three contributing terms to the total BRF of the vegetation layer, $\rho_{coupled}^{total}(z_{toc}, \Omega, \Omega_0)$ in (23), the implementation of the inverse mode requires estimating the ρ_0 values for all canopy conditions predefined by vectors **B**, **O** and **S**, and all $\mathcal{N}$ available spectral bands:

$$\overline{\rho}_0 = \frac{\sum_i W_{\rho_0}(i)\left[\rho_{data}(z_{toc}, i) - \rho_{veg}^{Coll}(z_{toc}, i; \mathbf{B}, \mathbf{O}, \mathbf{S}, LAI_{scene})\right]}{\sum_i W_{\rho_0}(i)\,\breve{\rho}_{bgd}^{total}\left(z_{toc}, i; \mathbf{B}, \tilde{\mathbf{O}}, \mathbf{S}, LAI_{scene}, \widetilde{LAI}_{scene}, k, \Theta, \rho_0\right)} \tag{28}$$

with

$$\begin{aligned}\breve{\rho}_{bgd}^{total}&\left(z_{toc}, i; \mathbf{B}, \tilde{\mathbf{O}}, \mathbf{S}, LAI_{scene}, \widetilde{LAI}_{scene}, k, \Theta, \rho_0\right)\\ &= \breve{\rho}_{bgd}^{UnColl}(z_{toc}, i; \mathbf{B}, \mathbf{S}, LAI_{scene}, k, \Theta)\\ &\quad + \breve{\rho}_{bgd}^{\|Coll}\left(z_{toc}, i; \mathbf{B}, \tilde{\mathbf{O}}, \widetilde{LAI}_{scene}, k, \Theta, \rho_0\right)\end{aligned} \tag{29}$$

and where the index i designates the angular measurement number in the available spectral set, and $W_{\rho_0}(i)$ is a weighting function that can be set equal to unity or any other value maximizing the impact of measurement i in the retrieval, as appropriate. Since the angular function $\breve{\rho}_{bgd}^{total}(z_{toc}, i; \mathbf{B}, \tilde{\mathbf{O}}, \mathbf{S}, LAI_{scene}, \widetilde{LAI}_{scene}, k, \Theta, \rho_0)$ in (29) is a function of $\overline{\rho}_0$ an iteration procedure can be applied to solve (28) until the convergence criterion $|\overline{\rho}_0^{itn} - \overline{\rho}_0^{it(n+1)}| \leq 10^{-3}$ is satisfied. This step ends up with $\mathcal{N}\overline{\rho}_0$ values times the number of canopy conditions.

[60] The ensemble of retrievals, for the preselected conditions, is analyzed with a comparison of the values

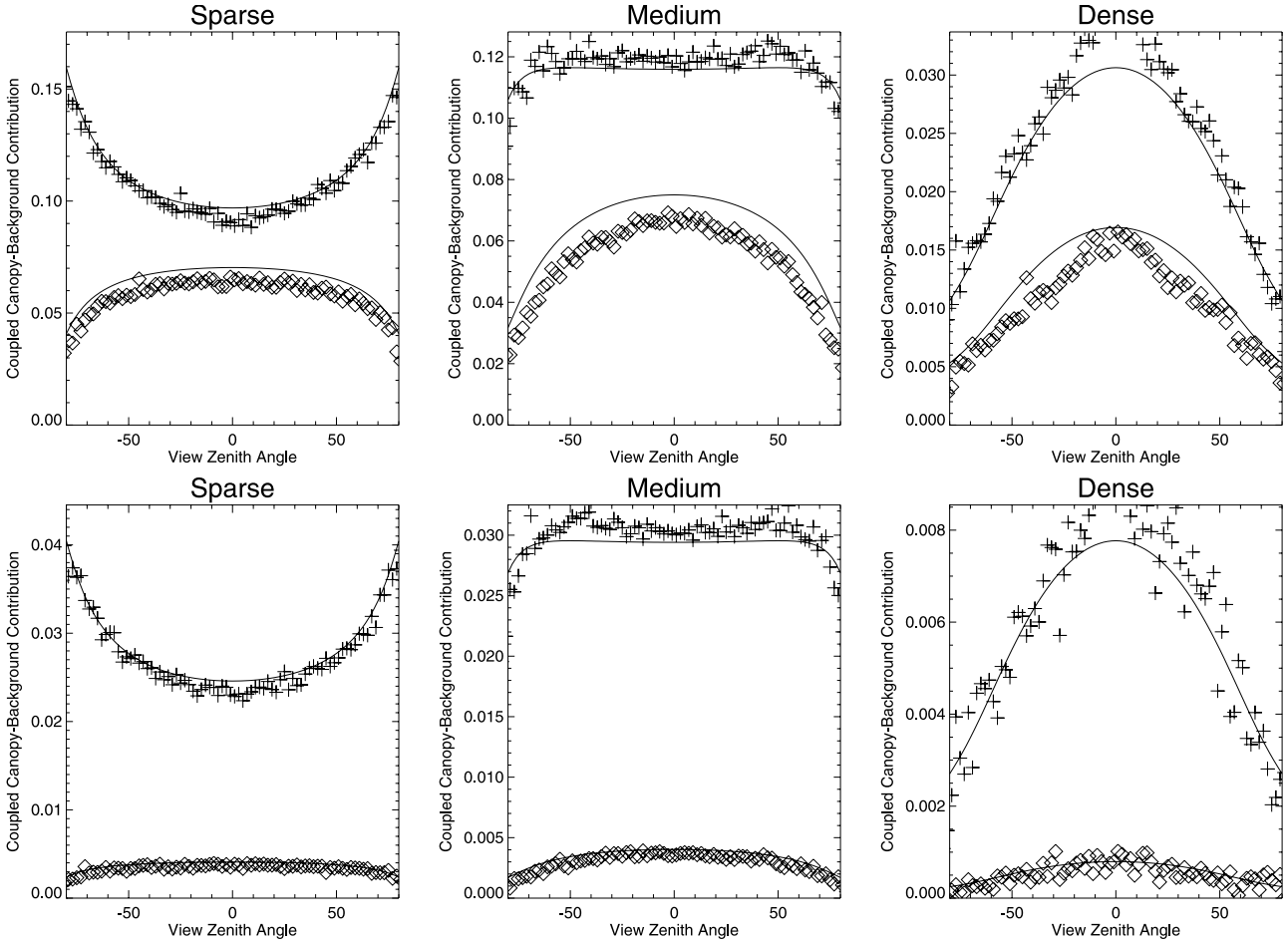

Figure 4. Same as Figure 3, except for the case of a Sun zenith angle of 60°.

obtained for the following $\chi^2(\lambda)$ metrics defining the cost function for all potential solutions:

$$\chi^2(\lambda) = \frac{\sum_i W_{\chi^2}(i,\lambda)\left[\rho_{data}(z_{toc},i,\lambda) - \rho^{total}_{coupled}(z_{toc},i,\lambda)\right]^2}{\sum_i W_{\chi^2}(i,\lambda)\,\sigma^2(i,\lambda)} \tag{30}$$

where $\rho^{total}_{coupled}(z_{toc}, i, \lambda)$ is a formal function of **B**, $\tilde{\mathbf{O}}$, **S**, LAI_{scene}, $\widetilde{LAI}_{scene}$, ρ_0, k and Θ. $W_{\chi^2}(i, \lambda)$ is a spectral weighting function, $\rho_{data}(z_{toc}, i, \lambda)$ is the ith angular measurement of the spectral BRF value at the top of the vegetation layer, and $\sigma^2(i, \lambda)$ is the assumed uncertainty in both the observation simulations and the actual spectral data. The weighting functions $W_{\chi^2}(i, \lambda)$ can be chosen so as to maximize the impact of the appropriate conditions of illumination and observation or wavelength and to optimize the relative contribution to the observation due to the terms mostly controlled by the variables being sought (for example, large view angles will enhance the contribution due to the LAI of the scene and, conversely, the close to nadir view conditions will enhance the background brightness effects); these settings, in turn, should convert into an increased accuracy in the retrievals of the variables of interest. Many simulation tests must be performed to optimize the weighting functions $W_{\chi^2}(i, \lambda)$ if so desired.

[61] Thus strictly speaking, only those coupled canopy and background conditions satisfying $\chi^2(\lambda) \leq 1.0$ for each and every $\mathcal{N}$ spectral bands with the condition that the canopy variables in vectors **B**, **S** remain unchanged across the spectral bands are eligible for being part of the set of "acceptable" solutions. Since the inversion will not yield the actual canopy and associated background conditions because of a series of ill-posed problems, the retrieval technique must ideally deliver a probability distribution function of the "acceptable" solutions chosen against the set of "possible" solutions, that can be screened to select the most "likely" solution and the uncertainty range related to the state variables of interest [e.g., *Pinty et al.*, 2000b]. Since the set of "possible" solutions admit discrete values in vectors **B**, **S**, and **O**, the proper evaluation of these uncertainties impose constraints on the discretization strategy adopted to generate the LUTs.

[62] In order to limit the consequences of such ill-posed and somewhat poorly conditioned inverse problem, the selection of the "likely" solution can take advantage of some heuristic knowledge. The latter could capitalize on various aspects such as, for instance, that the canopy structure of evergreen boreal forests is not expected to change significantly during strong local climate-driven transition yielding, by contrast, the background properties to change drastically (snow deposition and melting, for instance). Therefore, in the case of evergreen biome types

whose radiation transfer regimes are very sensitive to structure, the accumulation of measurements acquired during multiple satellite orbits over changing background conditions should translate into a better conditioning of the inversion.

[63] Many options can be envisaged regarding these aspects of the retrieval technique. They do require extensive testing to be performed under controlled, that is model-simulated, environments. These issues and a detailed analysis of the results delivered by inversion of (23) and (24) against time series of multiangle and multispectral measurements are actively investigated.

5. Concluding Remarks

[64] The proposed inversion technique focuses on the retrieval of vegetation canopy parameters for structurally heterogeneous systems overlying an anisotropic spatially uniform surface background. The radiance fields emerging at the top of such three-dimensional systems is first decomposed into three separate contributions, namely, the ''Black Background,'' the ''Black Canopy,'' and the remaining radiance field resulting from the radiation multiply scattered by both the vegetation layers and the background. Such a decomposition facilitates the decoupling of the radiative effects intrinsic to the vegetation layers from those involving the anisotropic background. These background properties are specified using a parametric BRF model whose unique mathematical feature includes expressing this BRF as the product of the background brightness by an ad hoc angular function. The decomposition of the total radiance fields emerging at the top of the three-dimensional system is thus performed in such a way that the wavelength-independent contribution is isolated.

[65] It becomes therefore relevant to create a limited set of LUTs for representing both the ''Black Background'' and ''Black Canopy'' contributions. The latter can be estimated on the basis of accurate 3-D radiation transfer models for any desired and appropriate canopy structure scenario. By contrast, the remaining contribution is approximated in the limit case of an equivalent plane-parallel turbid medium situation. Since this equivalent representation should, as well, be formulated such that the intrinsic vegetation layers and anisotropic background effects are decoupled at best, we derive an extremely accurate parameterization of a 1-D model that capitalizes on developments made earlier by the cloud physics community. The equivalent 1-D approach imposes, however, to estimate effective values for the state variables in order to ensure a radiatively consistent and accurate reconstruction of the radiant fluxes and radiance fields.

[66] The approach proposed to estimate the effective values of the state variables is quite straightforward and capitalizes on the availability of accurate Monte-Carlo ray tracing simulations of the ''Black Background'' and ''Black Canopy'' contributions. It also benefits from a specific vegetation feature, namely, that the extinction coefficient does not depend on the wavelength. This feature permits us separating the estimate of the effective LAI value from those of the variables describing the leaf scattering properties; the effective LAI value is indeed derived from an analysis of the ''Black Canopy'' contribution, while the effective leaf reflectance and transmittance values are estimated from an inversion of the 1-D turbid medium ''Black Background'' model against its analogous ''Black Background'' contribution generated by the 3-D model. The effective LAI value is always lower than the domain-averaged LAI values of the ''radiatively independent volumes'' and the LAI reduction factor lies in between approximately 0.3 for the low density and 0.8 for the high density scenarios. Under these conditions, the effective leaf single scattering albedo is found to be approximately 12 to 18% smaller than the corresponding actual values in the near-infrared spectral domain. Additional simulation studies are needed to properly identify the role of the woody elements versus the leaves in the assessment of the effective variable values. In the present study, the effective values incorporate the contributions due to the stems and trunks.

[67] Alternate approaches for assessing the effective values, based on a more insightful and theoretical analysis of the radiative effects induced by spatial heterogeneity, can certainly be envisaged in further studies. As compared to the cloud problem, the vegetation problem has the advantage that the assessment of the effective values can be performed separately for the canopy LAI and optical properties. The crux of the vegetation problem remains in the statistical representation of the gaps that may or may not follow standard distribution laws, depending on a number of anthropogenic, climatic, and ecological factors as well as the size of the ''radiatively independent volume.''

[68] The proposed decomposition of the total radiance field that merges various tools and aspects of three dimensional radiation transfer in heterogeneous systems proves to be very accurate with respect to the results obtained by Monte-Carlo ray tracing simulations under a variety of average and extreme conditions. The inversion scheme requires three separate steps consisting in (1) the estimation of the background brightness for each of the predefined canopy scenarios forming the set of possible solutions, (2) the delineation of a subset containing the acceptable solutions, and (3) the selection of the most likely solution.

[69] Since this inversion scheme is not suffering from the many technical constraints imposed by operational applications including data staging, the selection of the likely solution and the uncertainty ranges associated with the most prominent state variables can benefit from the availability of the entire multiangle and multispectral data archive. A detailed analysis of the results of numerous simulations is ongoing to determine the applicability of this approach.

[70] **Acknowledgments.** This research would not have been possible without the support of the Global Vegetation Monitoring unit of the Institute for Environment and Sustainability at the Joint Research Centre, an institution of the European Commission. The stimulating exchanges of ideas with other scientific communities, in particular with the cloud physics community, are also gratefully acknowledged.

References

Borel, C. C., S. A. W. Gerstl, and B. J. Powers (1991), The radiosity method in optical remote sensing of structured 3-D surfaces, *Remote Sens. Environ.*, *36*, 13–44.

Cahalan, R. F., and J. B. Snider (1989), Marine stratocumulus structure, *Remote Sens. Environ.*, *28*, 95–107.

Cahalan, R. F., W. Ridgway, W. J. Wiscombe, T. L. Bell, and J. B. Snider (1994), The albedo of fractal stratocumulus clouds, *J. Atmos. Sci.*, *51*, 2434–2455.

Cairns, B., A. Lacis, and B. Carlson (2000), Absorption within inhomogeneous clouds and its parameterization in general circulation models, *J. Atmos. Sci.*, *57*, 700–714.

Cescatti, A. (1988), Effects of needle clumping in shoots and crowns on the radiative regime of a Norway Spruce canopy, *Ann. Sci. For.*, *55*, 89–102.

Chandrasekhar, S. (1960), *Radiative Transfer*, 393 pp., Dover, Mineola, N. Y.

Engelsen, O., B. Pinty, M. M. Verstraete, and J. V. Martonchik (1996), Parametric bidirectional reflectance factor models: Evaluation, improvements, and applications, *Tech. Rep. EUR 16426 EN*, Joint Res. Cent., Eur. Comm., Ispra, Italy.

Gerard, F. F., and P. R. J. North (1997), Analyzing the effect of structural variability and canopy gaps on forest BRDF using a geometric-optical model, *Remote Sens. Environ.*, *62*, 46–62.

Gerstl, S. A. W., and C. C. Borel (1992), Principles of radiosity method versus radiative transfer for canopy reflectance modeling, *IEEE Trans. Geosci. Remote Sens.*, *30*, 271–275.

Gobron, N., and D. Lajas (2002), A new inversion scheme for the RPV model, *Can. J. Remote Sens.*, *28*, 156–167.

Gobron, N., B. Pinty, and M. M. Verstraete (1997a), Theoretical limits to the estimation of the leaf area index on the basis of optical remote sensing data, *IEEE Trans. Geosci. Remote Sens.*, *35*, 1438–1445.

Gobron, N., B. Pinty, M. M. Verstraete, and Y. Govaerts (1997b), A semidiscrete model for the scattering of light by vegetation, *J. Geophys. Res.*, *102*, 9431–9446.

Govaerts, Y. (1996), A model of light scattering in three-dimensional plant canopies: A Monte Carlo ray tracing approach, *EUR Rep. 16394 EN*, Space Appl. Inst., Ispra, Italy.

Govaerts, Y., and M. M. Verstraete (1998), Raytran: A Monte Carlo ray tracing model to compute light scattering in three-dimensional heterogeneous media, *IEEE Trans. Geosci. Remote Sens.*, *36*, 493–505.

Gurney, K. R., et al. (2002), Towards robust regional estimates of CO_2 sources and sinks using atmospheric transport models, *Nature*, *415*, 626–630.

Jupp, D. L. B., and A. H. Strahler (1991), A hot spot model for leaf canopies, *Remote Sens. Environ.*, *38*, 193–210.

Knorr, W., and M. Heimann (2001), Uncertainties in global terrestrial biosphere modeling: 2. Global constraints for a process-based vegetation model, *Global Biogeochem. Cycles*, *15*, 227–246.

Knyazikhin, Y. V., and A. L. Marshak (1991), Fundamental equations of radiative transfer in leaf canopies, and iterative methods for their solution, in *Photon-Vegetation Interactions*, edited by R. Myneni and J. Ross, pp. 9–43, Springer-Verlag, New York.

Knyazikhin, Y. V., A. L. Marshak, and R. B. Myneni (1992), Interaction of photons in a canopy of finite-dimensional leaves, *Remote Sens. Environ.*, *39*, 61–74.

Knyazikhin, Y., J. Kranigk, R. B. Myneni, O. Panfyorov, and G. Gravenhorst (1998a), Influence of small-scale structure on radiative transfer and photosynthesis in vegetation canopies, *J. Geophys. Res.*, *103*, 6133–6144.

Knyazikhin, Y., J. V. Martonchik, D. J. Diner, R. B. Myneni, M. M. Verstraete, B. Pinty, and N. Gobron (1998b), Estimation of vegetation canopy leaf area index and fraction of absorbed photosynthetically active radiation from atmosphere-corrected MISR data, *J. Geophys. Res.*, *103*, 32,239–32,256.

Knyazikhin, Y., J. V. Martonchik, R. B. Myneni, D. J. Diner, and S. W. Running (1998c), Synergistic algorithm for estimation of vegetation canopy leaf area index and fraction of absorbed photosynthetically active radiation from MODIS and MISR data, *J. Geophys. Res.*, *103*, 32,257–32,276.

Knyazikhin, Y. V., A. L. Marshak, and R. B. Myneni (2004), Three-dimensional radiative transfer in vegetation canopies, in *Three-Dimensional Radiative Transfer in the Cloudy Atmosphere*, edited by A. Davis and A. Marshak, Springer-Verlag, New York.

Kuusk, A. (1991), The hot spot effect in plant canopy reflectance, in *Photon-Vegetation Interactions*, edited by R. Myneni and J. Ross, pp. 139–159, Springer-Verlag, New York.

Lenoble, J. (1985), *Radiative Transfer in Scattering and Absorbing Atmospheres: Standard Computational Procedures*, 300 pp., A. Deepak, Hampton, Va.

Liou, K. N. (1980), *An Introduction on Atmospheric Radiation*, 392 pp., Academic, San Diego, Calif.

Marshak, A. L. (1989), The effect of the hot spot on the transport equation in plant canopies, *J. Quant. Spectrosc. Radiat. Transfer*, *42*, 615–630.

Marshak, A. L., and A. Davis (2004), Horizontal fluxes and radiative smoothing, in *Three-Dimensional Radiative Transfer in the Cloudy Atmosphere*, edited by A. Davis and A. Marshak, Springer-Verlag, New York.

Marshak, A. L., A. Davis, R. F. Cahalan, and W. J. Wiscombe (1995), Radiative smoothing in fractal clouds, *J. Geophys. Res.*, *100*, 26,247–26,261.

Martonchik, J. V., D. J. Diner, R. A. Kahn, T. P. Ackerman, M. M. Verstraete, B. Pinty, and H. R. Gordon (1998), Techniques for the retrieval of aerosol properties over land and ocean using multiangle imaging, *IEEE Trans. Geosci. Remote Sens.*, *36*, 1212–1227.

Martonchik, J. V., B. Pinty, and M. M. Verstraete (2002), Note on an improved model of surface BRDF-atmospheric coupled radiation, *IEEE Trans. Geosci. Remote Sens.*, *40*, 1637–1639.

Nilson, T. (1971), A theoretical analysis of the frequency of gaps in plant stands, *Agric. Meteorol.*, *8*, 25–38.

Nilson, T. (1991), Approximate analytical methods for calculating the reflection functions of leaf canopies in remote sensing applications, in *Photon-Vegetation Interactions*, edited by R. B. Myneni and J. Ross, pp. 163–189, Springer-Verlag, New York.

Nilson, T., and A. Kuusk (1989), A reflectance model for the homogeneous plant canopy and its inversion, *Remote Sens. Environ.*, *27*, 157–167.

Oker-Blom, P., and S. Kellomaki (1983), Effect of grouping of foliage on the within-stand and within-crown light regime: Comparison of random and grouping models, *Agric. Meteorol.*, *28*, 143–155.

Oreopoulos, L., A. Marshak, R. F. Cahalan, and G. Wen (2000), Cloud three-dimensional effects evidenced in Landsat spatial power spectra and autocorrelation functions, *J. Geophys. Res.*, *105*(D11), 14,777–14,788.

Panferov, O., Y. Knyazikhin, R. B. Myneni, J. Szarzynski, E. Engwald, K. G. Schnitzler, and G. Gravenhorst (2001), The role of canopy structure in the spectral variation of transmission and absorption of solar radiation in vegetation canopies, *IEEE Trans. Geosci. Remote Sens.*, *39*, 241–253.

Petty, G. W. (2002), Area-average solar radiative transfer in three-dimensional inhomogeneous clouds: The independently scattering cloudlet model, *J. Atmos. Sci.*, *59*, 2910–2929.

Pinty, B., and M. M. Verstraete (1998), Modeling the scattering of light by vegetation in optical remote sensing, *J. Atmos. Sci.*, *55*, 137–150.

Pinty, B., M. M. Verstraete, and N. Gobron (1998), Impact of soil anisotropy on the radiance field emerging from vegetation canopies, *Geophys. Res. Lett.*, *25*, 797–800.

Pinty, B., F. Roveda, M. M. Verstraete, N. Gobron, Y. Govaerts, J. Martonchik, D. Diner, and R. Kahn (2000a), Surface albedo retrieval from METEOSAT: 1. Theory, *J. Geophys. Res.*, *105*, 18,099–18,112.

Pinty, B., F. Roveda, M. M. Verstraete, N. Gobron, Y. Govaerts, J. Martonchik, D. Diner, and R. Kahn (2000b), Surface albedo retrieval from METEOSAT: 2. Application, *J. Geophys. Res.*, *105*, 18,113–18,134.

Pinty, B., et al. (2001), The Radiation Transfer Model Intercomparison (RAMI) exercise, *J. Geophys. Res.*, *106*, 11,937–11,956.

Pinty, B., J.-L. Widlowski, N. Gobron, M. M. Verstraete, and D. J. Diner (2002), Uniqueness of multiangular measurements - Part 1: A subpixel surface heterogeneity indicator from MISR, *IEEE Trans. Geosci. Remote Sens.*, *40*, 1560–1573.

Pinty, B., et al. (2004), The Radiation Transfer Model Intercomparison (RAMI) exercise: Results from the second phase, *J. Geophys. Res.*, *109*, D06210, doi:10.1029/2003JD004252.

Prusinkiewicz, P., and A. Lindenmayer (1990), *The Algorithmic Beauty of Plants*, 240 pp., Springer-Verlag, New York.

Rahman, H., B. Pinty, and M. M. Verstraete (1993), Coupled surface-atmosphere reflectance (CSAR) model: 2. Semiempirical surface model usable with NOAA Advanced Very High Resolution Radiometer data, *J. Geophys. Res.*, *98*, 20,791–20,801.

Rautiainen, M., P. Stenberg, T. Nilson, and A. Kuusk (2004), The effect of crown shape on the reflectance of coniferous stands, *Remote Sens. Environ.*, *89*, 41–52.

Rayner, P. J., I. G. Enting, R. J. Francey, and R. Langenfelds (1999), Reconstructing the recent carbon cycle from atmospheric CO_2, *Tellus, Ser. B*, *51*, 213–232.

Ross, J. (1981), *The Radiation Regime and Architecture of Plant Stands*, 391 pp., W. Junk, Boston, Mass.

Shultis, J. K., and R. B. Myneni (1988), Radiative transfer in vegetation canopies with anisotropic scattering, *J. Quant. Spectrosc. Radiat. Transfer*, *39*, 115–129.

Strahler, A. H., and D. L. B. Jupp (1991), Geometric-optical modeling of forests as remotely sensed scenes composed of three-dimensional discrete objects, in *Photon-Vegetation Interactions*, edited by R. B. Myneni and J. Ross, pp. 417–439, Springer-Verlag, New York.

Szczap, F., H. Isaka, M. Saute, B. Guillemet, and A. Ioltukhovski (2000), Effective radiative properties of bounded cascade absorbing clouds: Definition of an effective single-scattering albedo, *J. Geophys. Res.*, *105*, 20,635–20,648.

Tian, Y., Y. Wang, Y. Zhang, Y. Knyazikhin, J. Bogaert, and R. B. Myneni (2002), Radiative transfer based scaling of LAI retrievals from reflectance data of different resolutions, *Remote Sens. Environ.*, *84*, 143–159.

Titov, G. (1990), Statistical description of radiation transfer in clouds, *J. Atmos. Sci.*, *47*, 24–38.

Titov, G. (1998), Radiative horizontal transport and absorption in stratocumulus clouds, *J. Atmos. Sci.*, *55*, 2549–2560.

Verstraete, M. M., B. Pinty, and R. E. Dickinson (1990), A physical model of the bidirectional reflectance of vegetation canopies: 1. Theory, *J. Geophys. Res.*, *95*, 11,765–11,775.

Welles, J. M., and J. M. Norman (1991), Photon transport in discontinuous canopies: A weighted random approach, in *Photon-Vegetation Interactions*, edited by R. B. Myneni and J. Ross, pp. 391–413, Springer-Verlag, New York.

Widlowski, J.-L. (2002), Extracting quantitative subpixel heterogeneity information from optical remote sensing data, *Rep. EUR 20236 EN*, Joint Res. Cent., Ispra, Italy.

Widlowski, J.-L., B. Pinty, N. Gobron, M. M. Verstraete, and A. B. Davies (2001), Characterization of surface heterogeneity detected at the MISR/TERRA subpixel scale, *Geophys. Res. Lett.*, *28*, 4639–4642.

Widlowski, J.-L., M. M. Verstraete, B. Pinty, and N. Gobron (2003), Allometric relationships of selected European tree species, *Rep. EUR 20855 EN*, Joint Res. Cent., Ispra, Italy.

Widlowski, J.-L., B. Pinty, N. Gobron, M. M. Verstraete, D. J. Diner, and A. B. Davis (2004), Canopy structure parameters derived from multiangular remote sensing data for terrestrial carbon studies, *Clim. Change*, in press.

N. Gobron, T. Lavergne, B. Pinty, M. M. Verstraete, and J.-L. Widlowski, Global Vegetation Monitoring Unit, IES, EC Joint Research Centre, TP 440, via E. Fermi, I-21020 Ispra (VA), Italy. (bernard.pinty@jrc.it)